Effects of Pulse Delay in Metal Micromachining with Femtosecond Laser Pulses

Jaegu KIM[*], Sunghak CHO[*], Wonseok CHANG[*], Suckjoo NA[**] and Kyunghyun WHANG[*]

[*]*Nanomachining team, Korea Institute of Machinery & Materials,*
171 Jang-dong Yusong-ku, Daejeon 305-343, South Korea
E-mail: gugu99@kimm.re.kr
[**] *Korea Advanced Institute of Science and Technology, 373-1 Guseong-dong Yusong-ku,*
Daejeon 305-701, South Korea

Single and double femtosecond laser pulses with different time delays were used to investigate surface morphology changes in Cr thin films. A double pulse was generated by varying the beam path length of a split pulse and recombining the two beams. With a single pulse, a nanometer-sized droplet was formed on the irradiated surface; the area was dependent on the laser power. With multiple pulses at a fixed repetition rate, the subwavelength ripples aligned perpendicular to the polarization direction of the laser light with a spacing of about 200 nm. Curiously, the initial ripple was in the same direction as the laser polarization for the first few pulses. Using a double pulse with different polarization directions and a time separation of zero, the ripples formed in the sum vector direction of both beams. Increasing the time separation removed the ripples effectively. After a few tens of ps, the second pulse did not affect the surface changes. The changes in surface morphology were attributable to interference or disturbances between the hot electron oscillations induced by the two pulses and the diffusion time of the electron energy. A double pulse with different polarization directions within the diffusion time of the electron energy is a useful method for decreasing the size of the ablated area and eliminating ripples in micromachining.

DOI: 10.2961/jlmn.2007.01.0015

Keywords: femtosecond laser, micromachining, Cr film ablation, surface ripple, time delay

1. Introduction

Femtosecond direct laser micromachining is a very useful tool for industrial applications and research. The characteristic high peak power of femtosecond pulse laser machining resulting from the ultrashort temporal pulse width can minimize the heat effect zone (HAZ) and produce nonlinear effects. For the same reason, it can be used to fabricate diffraction-limit-sized objects using power just above the upper threshold value [1]. Although a smaller feature size has the advantage of increasing the spatial resolution in machining, it is difficult to keep the laser energy of a single pulse steady over the long term while machining a large area. Furthermore, when a metal thin is film irradiated at a high pulse energy, thermal damage occurs on the substrate at below the boiling temperature, and much debris spreads over the sample. Therefore, to obtain high-quality machining with minimal thermal damage, the sample should be machined at near the threshold energy using irradiation with multiple pulses. However, at near the ablation threshold energy using multiple pulses, a periodic surface pattern called a laser-induced periodic surface structure (LIPPS), or ripples, occurs in various materials [2–5], which is a negative phenomenon in subtractive micromachining. The ripples in a metal sample irradiated with a femtosecond laser pulse form as a result of the thermal equilibrium between the hot electrons and the surrounding lattice and are affected by the interaction between the following pulse and the surface properties already formed by the previous pulse.

In this study, to elucidate the process of ripple formation we investigate the thermal effects on a Cr metal thin surface of a femtosecond laser with a single high-energy pulse and the dynamic surface changes produced by a double pulse with a varying time delay.

The micromachining of a metallic thin film on plain glass is widely used in fields such as mask repairing for semiconductors and in micro-electromechanical and optical devices, etc.

2. Experiments

The laser system used in the experiment was an amplified Ti:sapphire laser with a pulse duration of 250 fs full width at half-maximum (FWHM) with linear polarization, a maximum power of 500 mW at a repetition rate of 100 kHz, and a wavelength of 800 nm. To produce a double pulse, a Michelson interferometer was modified and the pulse energy and polarization were varied using a half-wave plate and polarizer. One of the two pulses was delayed by controlling the optical path length using an accurate motion stage with a resolution of 0.1 μm, as shown in Fig. 1. A two-photon excited photodiode was used to determine a time delay of zero for each pulse.

We used a magnification microscope objective IR lens (×100, NA 0.8; Olympus) with an XYZ stage for accurate positioning. The incident beam was at an angle of 90° to the sample. To adjust the number of pulses, we used a mechanical shutter and adjusted the shutter on/off time using a PC-based controller. In case of number up to 200 pulses, we used the pulse generator to trigger the cavity dumper.

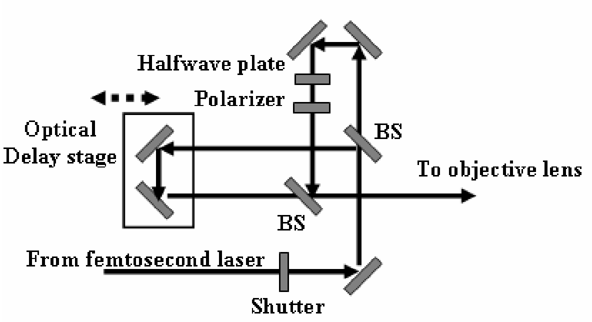

Fig. 1 Schematic diagram of the experimental system

The experiments were performed in air at ambient pressure and temperature. We used sputtering to fabricate Cr thin films with an average thickness of 200 nm on a glass substrate. The workpiece was cleaned with methanol before placing it on the stage without considering the formation of oxide layer on metal surface. We used scanning electron microscopy (SEM) to observe the surface morphology.

3. Experimental results and discussion

3.1 Single pulse irradiation

The ablation on a 200-nm-thick Cr thin film following a single shot is shown in Fig. 2. In the case of a single 3.5 nJ pulse, we observed pure melting, in which initial droplets with a diameter of several tens of nanometers were created on the surface. The creation of these droplets may have been due to the surface tension that occurs during the resolidification of molten material. This characteristic has been observed with other laser sources and different samples [6,7]. Although the material removal process can be explained by surface evaporation or volumetric phase expulsion, no substantial surface or volume was evaporated from the melted surface at this energy level. The very low energy seemed to merely melt the surface, which then solidified.

On irradiation with subsequent pulses at a repetition rate of 100 kHz, the subwavelength ripples appeared perpendicular to the polarization direction of the laser light and had a spacing of ~200 nm. We interpret the differences of a ~500 nm spacing from previous experiments [8] might be caused by the oxide layer or the tight focusing. Interestingly, however, the initial ripples were in the same direction as the polarization, and formed when the surface was just melting, as shown in Fig. 2(b). Similar results were observed for irradiation energies of 4.3 and 4.6 nJ with five pulses, as shown in Fig. 3(a) and (b). These results and mechanism are under investigated.

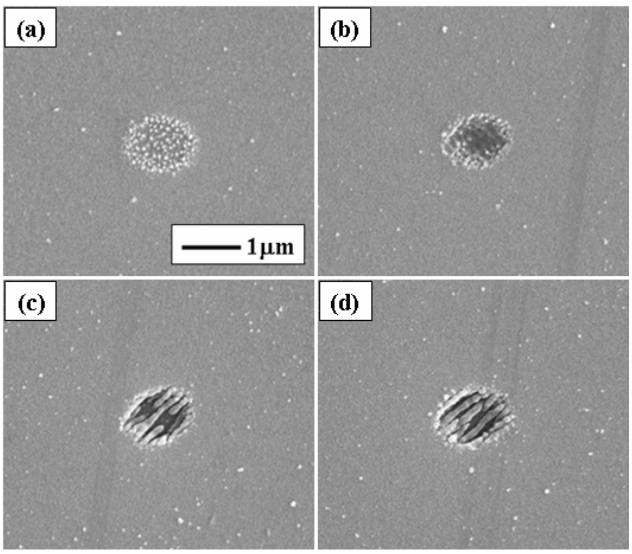

Fig. 2 Ablation pattern at an energy of 3.5 nJ with (a) 1, (b) 5, (c) 20, and (d) 200 pulses

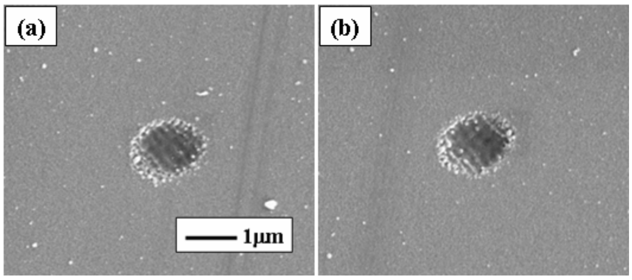

Fig. 3 Ripples aligned parallel to the direction of the electric field at energies of (a) 4.3 and (b) 4.6 nJ with five pulses

The damage threshold energy can be obtained from the experimental results. As the power distribution of the spatial beam profile is Gaussian, as shown in Fig. 4, the threshold energy (P_c) and beam radius (w) are expressed for each power (P_1 and P_2) and damage radius (r_1 and r_2) as

$$P_c = \exp\left(\frac{\ln P_2 - \left(\frac{r_2}{r_1}\right)^2 \ln P_1}{1 - \left(\frac{r_2}{r_1}\right)^2} \right) \tag{1}$$

and

$$w = \frac{r_1}{\sqrt{\frac{1}{2}\ln\frac{P_1}{P_c}}} \tag{2}$$

From this calculation, we obtained a damage threshold

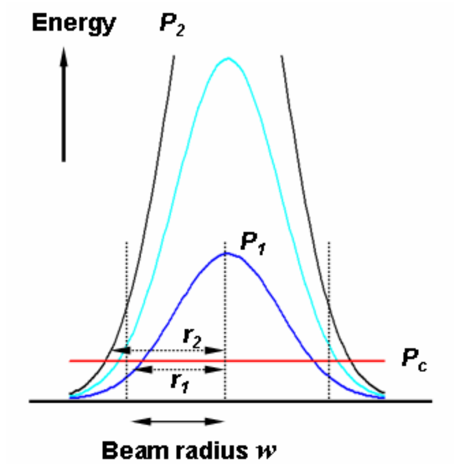

Fig. 4 Calculating the threshold energy and beam radius from the two experimental results assuming that the spatial beam profile has a Gaussian distribution

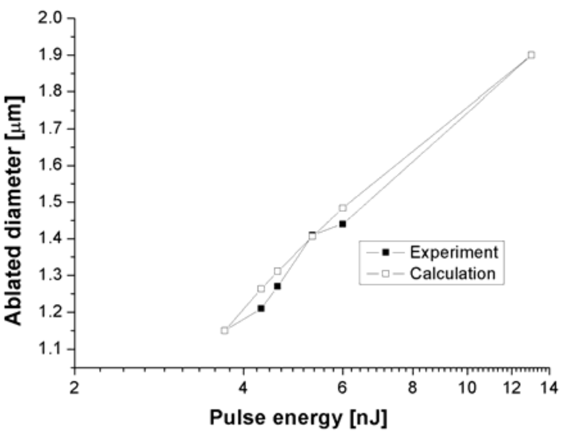

Fig. 5 Comparison of the diameter of the ablated area in experiment and the calculation based on Eq. (1) and (2)

energy of 1.8 nJ and an incident beam diameter of 1.9 μm; therefore, the threshold fluence was about 60 mJ/cm^2. The diameter obtained from the calculation based on the experimental results was larger than 1.22 μm based on diffraction given as $d = 2.44\lambda f\#$, where λ is the wavelength and $f\#$ is the f-number. However, it is reasonable to calculate the fluence of the damage threshold using the energy value obtained from Equations (1) and (2) due to the good agreement between the experimental results and the calculation, as shown in Fig. 5.

3.2 Double pulses varying time delay

Figure 6 shows the surface morphology with 10,000 pulses at energies of 0.44 and 0.4 nJ having different polarization directions and time delays ranging from 0 to 50 ps between split pulses. Although the calculated damage threshold from section 3.1 was 1.8 nJ, we observed damage at a pulse energy of about 0.4 nJ, reflecting the thermal incubation effect. The ablated feature was smaller than the wavelength with multiple irradiation by a single pulse at an energy of 0.44 nJ, as shown in Fig. 6(a). However, prominent ripples did not appear.

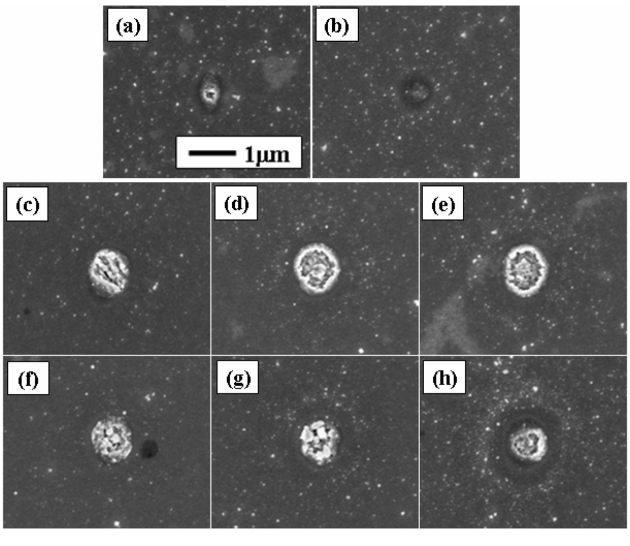

Fig. 6 Ablation of a Cr thin film with 10,000 pulses. (a) 0.44 nJ/pulse and vertical polarization, and (b) 0.4 nJ/pulse and horizontal polarization. The time delay between (a) and (b) was (c) 0, (d) 0.5, (e) 1, (f) 10, (g) 30, and (h) 50 ps.

When a split pulse irradiated the sample at the same time, the ripples appeared in the direction of the sum vector of each pulse, as shown in Fig. 6(c). As the time separation increased, the ripples disappeared and the irradiated area became clean (Fig. 6(d) and (e)). With a time separation greater than 10 ps, fragments or debris were present in the irradiated area (Fig. 6(f) and (g)). As the separation reached 50 ps, the diameter of the machined area became smaller.

Based on these results, we postulated on the cause of the dynamic change in ripple formation according to the time variation. Ripple formation is thought to arise from the interference between incident wave and surface scattering wave at near the threshold energy. The spacing of the ripples is dependent on the wavelength and the incident angle expressed as $\Lambda = \lambda/(1 \pm \sin\theta_i)$. However, subwavelength spacing that does not agree with this equation has been observed [5,9–11]. Since the ripples in metal are generally based on lattice reordering caused by lattice movement with the thermal energy distribution and by resolidification, the process from the laser energy to lattice disordering should be defined.

The laser energy transferred to the material involves absorption via inverse Bremsstrahlung, electron–electron thermalization, and electron–phonon coupling [12]. The two-temperature model is widely used to analyze the transient electron and lattice temperature [13] and represents how much of the laser radiation is absorbed by electrons and heat diffusion to the lattice subsystem. The electrons absorb the laser energy and then transfer it to the lattice via electron–lattice coupling. This coupling constant and hot electron diffusion, which are related to the final hot electron temperature, are the dominant factors causing surface melting and ripple formation in metals [8].

Therefore, the change in the ripple with the temporal separation of pulses is interpreted as being dependent on the electron temperature followed by the lattice temperature according to the two-temperature model and surface morphology observations. Furthermore, we must consider hot electron density oscillation, such as surface electromagnetic waves generated by the interface layer between dielectric material and metal or Langmuir waves, before the electron energy diffuses into the lattice. These waves may lead to spatial energy modulation of hot electron. The subsequent pulse also causes hot electron oscillation, which interferes with the existing electron oscillation induced by the previous pulse unless the previous hot electron energy has diffused into the lattice resulting in lattice disorder. Otherwise, it interferes with the lattice via the diffusion of electron energy, and these results in ripples oriented perpendicular to the direction of the electric field, as shown in Fig. 2. Therefore, electron oscillation is affected by the second pulse in a different polarization direction when the electrons are irradiated within the diffusion time of the hot electron energy. Finally, the total disturbed hot electron temperature defines the surface morphology and ablation area. This interpretation is in good agreement with the experimental results shown in Fig. 6(c)–(h). Similar electron behavior with the time lapse after excitation with a femtosecond laser pulse is found in fused silica samples [14].

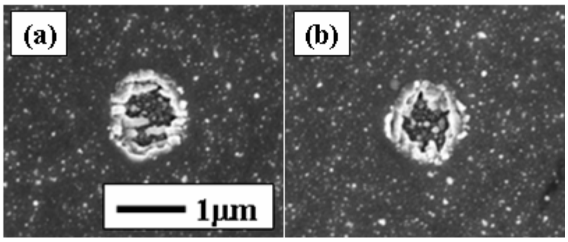

Fig. 7 Ablation on a Cr thin film with 10,000 pulses and a single pulse energy of (a) 1.4 nJ and vertical polarization and (b) 1.3 nJ and horizontal polarization

In addition to eliminating the ripples, another advantage of a double pulse separated by 0.5 to 1 ps is that it allows machining of a smaller area with a lower energy. As shown in Fig. 7(a) and (b), ripples at the outer edge were generated at higher energies of 1.4 and 1.3 nJ and 10,000 pulses. However, machining with a double pulse with different polarization directions and a total energy of 0.84 nJ gave much better quality in terms of clearness and the size of the ablated area than that with an energy of 1.4 nJ, as shown in Fig. 6(d) or (e).

4. Conclusions

We investigated the surface morphology of Cr thin films, using a tightly focused spot size and single and time-delayed femtosecond laser pulses. With a single pulse, a surface droplet was observed. We interpret this as resulting from the surface tension of melted material in the process of resolidification. Subwavelength ripples occurred when the surface was irradiated with multiple pulses, although curiously, with only a few pulses the ripples aligned parallel to the laser polarization direction. From calculations based on the experimental results for a single pulse, we obtained a damage threshold energy of 1.8 nJ and incident beam diameter of 1.9 μm; therefore, the threshold fluence was about 60 mJ/cm^2.

Based on observations of the surface morphology using a double pulse with time separations varying from 0 to 50 ps, the surface changes seemed to be dependent on the hot electron oscillation and its diffusion time into the lattice. Therefore, it was possible to eliminate the ripples using a double pulse with different polarization directions if the two pulses were not coincident and the second pulse occurred within the diffusion time of the hot electrons induced by the first pulse. Furthermore, it was possible to ablate the sample clean with less energy compared to using multiple higher-energy pulses with the same polarization. In the latter case, the ripples remained in the outer region and the diameter of the ablated area was large.

A double pulse with different polarization directions within the diffusion time of the electron energy is a useful method for decreasing the size of the ablated area and eliminating unwanted ripples in subtractive micromachining.

References

[1] F. Korte, S. Adams, A. Egbert, C. Fallnich, A. Ostendorf, S. Nolte, M. Will, J.-P. Ruske, B.N. Chichkov, and A. Tunnerrmann: Opt. Express. **7**, (2000) 41.

[2] D. Bauerle: "Laser Processing and Chemistry, 3rd Ed." (Springer, Berlin, 2000) p. 571

[3] J.E. Sipe, J.F. Young, J.S. Preston, and H. M. van Driel: Phys. Rev. B, **27**, (1983) 1141.

[4] M. Csete, and Zs. Bor: Appl. Surf. Sci., **133**, (1998) 5.

[5] A. Borowiec, and H. K. Haugen: Appl. Phys. Lett., **82**, (2003) 4462.

[6] J. Kruger, P. Meja, M. Autric, and W. Kautric: Appl. Surf. Sci., **186**, (2002) 374.

[7] S.K. Lee, K.K. Yoon, K.H. Whang, and S.J. Na: Surf. Coating. Tech., **113**, (1999) 63.

[8] J. Wang, and C. Guo: Appl. Phys. Lett., **87,** (2005) 251914.

[9] R. Wagner, J. Gottmann, A. Horn, and E. W. Kreutz: Appl. Surf. Sci., in press.

[10] Q. Wu, Y. Ma, R. Fang, Y. Liao, Q. Yu, X. Chen, and K. Wang: Appl. Phys. Lett., **82,** (2003) 1730.

[11] A.M. Ozkan, A.P. Malshe, T.A. Railkar, W.D. Brown, M.D. Shirk, and P.A. Molian: Appl. Phys. Lett., **75,** (1999) 3716.

[12] B. Rethfeld, A. Kaiser, M. Vicanek, and G. Simon: Phys. Rev. B, **65**, (2002) 214303.

[13] T.Q. Qiu, and C.L. Tien, Int. J. Heat Mass Transf., **35**, (1992) 719.

[14] I.H. Chowdhury, X. Xu, and A.M. Weiner, Appl. Phys. Lett., **86**, (2005) 151110.

(Received: May 16, 2006, Accepted: March 15, 2007)